World Journal of Engineering Research
Print ISSN: 2959-9865
Online ISSN: 2959-9873
DOI: https://doi.org/10.61784/wjer3045

DAY-AHEAD PREDICTIONS OF THE POWER GENERATED BY A PHOTOVOLTAIC POWER PLANT

JiGang Pan, Jie Qian*, MingLiang Cao
School of Mechanical and Electrical Engineering and Automation, Nanhang Jincheng College, Nanjing 211156, Jiangsu, China.
Corresponding Author: Jie Qian, Email: qjie4624@gmail.com

Abstract: As the proportion of renewable energy in the power grid continues to increase, accurate day-ahead photovoltaic (PV) power forecasting is critical for ensuring grid stability. This study proposes a systematic framework aimed at addressing four key challenges: a) introducing a two-dimensional bias matrix to quantify seasonal/intraday power fluctuation characteristics; b) establishing a rolling ridge regression model to achieve self-driven forecasting based on historical power data; c) innovatively designing a segmented strategy for sunny/cloudy/rainy weather scenarios to optimise the numerical weather prediction (NWP) fusion process, thereby addressing the variable meteorological impacts in practical applications and significantly improving prediction accuracy under complex meteorological conditions; d) employing weighted interpolation spatial downscaling techniques to refine NWP resolution to the power plant level. Validation results show that downscaling processing improved the Pearson correlation coefficient from 0.64 to 0.76, reduced the Root Mean Square Error (RMSE) from 0.57 kW to 0.46 kW, and decreased the Mean Absolute Error (MAE) from 0.49 kW to 0.34 kW. This integrated solution significantly enhances prediction accuracy, providing robust technical support for grid dispatch in high-penetration renewable energy systems and offering more reliable decision-making basis for smart grid management.
Keywords: Photovoltaic power prediction; Ridge regression; Numerical weather prediction; Spatial downscaling; Scenario segmentation

1 INTRODUCTION

Accurate next-day photovoltaic (PV) power generation forecasting is essential for maintaining grid stability as renewable energy penetration increases. The inherent intermittency and weather dependence of PV output present significant challenges for grid operators, making advanced forecasting methods a priority for research.

Recent literature demonstrates a range of approaches to improve PV power forecasting accuracy. Time series and machine learning models, including deep learning frameworks such as LSTM and hybrid CNN-GRU, have shown superior performance in capturing nonlinear and seasonal patterns in PV output, especially when combined with domain knowledge and feature selection techniques [1-5]. Weather scenario segmentation (clear/cloudy/rainy) and the integration of numerical weather prediction (NWP) data further enhance forecast precision under varying meteorological conditions [6-7]. Spatial downscaling and weighted interpolation methods refine NWP resolution to the plant level, improving the correlation and reducing forecast errors [6,7]. Additionally, optimization algorithms and unsupervised domain adaptation methods have been employed to address data scarcity and transferability across different PV sites [8-9]. The combination of physical and persistence models, especially when integrated with energy storage, also contributes to grid stability by managing ramp rates and power continuity [10].

The proposed systematic framework, which incorporates bias quantification, rolling regression, weather scenario segmentation, and spatial downscaling, addresses key challenges identified in the literature. By significantly improving forecast accuracy metrics such as Pearson correlation, RMSE, and MAE, this approach provides robust technical support for grid scheduling and stability in high-renewable systems. The integration of advanced data-driven and physical modeling techniques positions this research at the forefront of PV forecasting, offering practical solutions for real-world grid management.

2 PHOTOVOLTAIC POWER GENERATION FORECASTING MODEL FRAMEWORK AND EVALUATION INDEX ESTABLISHMENT

Photovoltaic power prediction analyzes irradiation-power statistical correlations by integrating historical data with NWP through multi-stage frameworks. This approach addresses meteorological, geographical, and seasonal fluctuations, overcoming traditional limitations from cloud transients and nonlinear thermal effects. Current advances prioritize dynamic feature engineering and scenario-adaptive mechanisms to resolve single-model generalization constraints.

2.1 Modeling Framework

Based on the purpose of this research, a block diagram of the process was constructed (shown in Figure 1).

© By the Author(s) 2025, under the CC BY-NC-ND license (http://creativecommons.org/licenses/by-nc-nd/4.0).

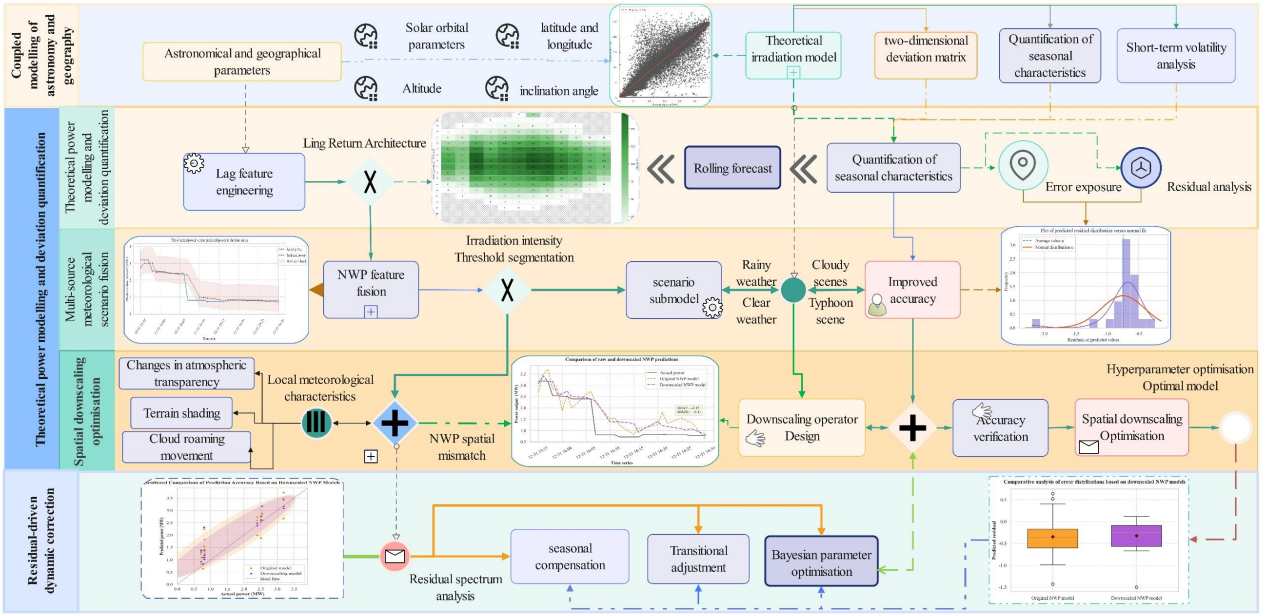

Figure 1 Flow Diagram

2.2 Description of Prediction Accuracy Evaluation

Considering the four-mode recursive format of this study, it is necessary to describe each indicator of its research accuracy separately.

Mean absolute error（MAE）：

$$MAE=\frac{1}{N}\sum_{i=1}^{N}|\Delta P(t_i)| \tag{1}$$

where $\Delta P(t_i)$ is the deviation of the actual value from the theoretical value

Root mean square error（RMSE）：

$$RMSE=\sqrt{\frac{1}{N}\sum_{i=1}^{N}\left(\Delta P(t_i)\right)^2} \tag{2}$$

Pearson correlation coefficient：

$$r=\frac{\sum_{i=1}^{N}(P_{act}(t_i)-\bar{P}_{act})(P_{theo}(t_i)-\bar{P}_{theo})}{\sqrt{\sum_{i=1}^{N}(P_{act}(t_i)-\bar{P}_{act})^2}\sqrt{\sum_{i=1}^{N}(P_{theo}(t_i)-\bar{P}_{theo})^2}} \tag{3}$$

where $\bar{P}_{act}$ is the actual observed power and $\bar{P}_{theo}$- is the theoretical power.

$$R^2=1-\frac{\sum_{j=1}^{M}[P(t_j)-\hat{P}(t_j)]^2}{\sum_{j=1}^{M}[P(t_j)-\bar{P}]^2} \tag{4}$$

Among them,

$$\bar{P}=\frac{1}{M}\sum_{j=1}^{M}P(t_j) \tag{5}$$

Mean absolute percentage error（MAPE）：

$$MAPE=\frac{100\%}{M}\sum_{j=1}^{M}\left|\frac{P(t_j)-\hat{P}(t_j)}{P(t_j)}\right| \tag{6}$$

3 PHOTOVOLTAIC POWER PREDICTION MODELING

3.1 Spatiotemporal Performance Diagnostic Model for PV Plants

Historical power-based PV plant analysis quantifies actual vs. theoretical power deviations using solar irradiation theory. A dual-scale (seasonal/diurnal) deviation model reveals spatiotemporal efficiency patterns, supporting prediction accuracy and grid stability enhancement.

3.1.1 Deviation calculation based on the generatable power model

In Mode 1, we constructed a deviation analysis model for "Theoretical Power Output - Actual Power Output" based on the irradiation intensity $G_{tilt}(t)$ of the inclined surface of the photovoltaic power station.

Theoretical power output mode. If the rated peak power of the photovoltaic module (under STC conditions) is P_{rated}, when doing normalization analysis, P_{rated} is often set to 1, and the standard irradiance is G_{STC} =1000 W/m^2, the theoretical output power at any given time t can be expressed as:

$$P_{theo}(t)=\frac{G_{tilt}(t)}{G_{STC}}=\frac{G_{tilt}(t)}{1000} \tag{7}$$

where P_{rated} is the rated peak power of the PV module, $G_{tilt}(t)$ is the tilt irradiance, $G_{STC}(t)$ is the standard irradiation level.

Let the actual observed power be denoted as $P_{act}(t)$. Then, the difference (deviation) between the two is

$$\Delta P(t)=P_{act}(t)-P_{theo}(t) \tag{8}$$

Quantifying seasonal and intraday characteristics Monthly average deviation Group the samples by month, and denote the set of time points contained in the m-th month (m = 1, ..., 12) as T_m, the average monthly deviation is then:

$$\overline{\Delta P_m}=\frac{1}{|T_m|}\sum_{t\in T_m}\Delta P(t) \tag{9}$$

where T_m={t:Month(t)=m} indicate the set of all time points t in a day that satisfy the m-th month.

$$\overline{\Delta P_h}=\frac{1}{|H_h|}\sum_{t\in H_h}\Delta P(t) \tag{10}$$

where $H_h=\{t:Hour(t)=h\}$, denote the set of all time points t in a day that satisfy the h-th month.

The two-dimensional deviation matrix is used to demonstrate this relationship in subsequent steps by means of the

$$D_{h,m}=\frac{1}{|\{t:Hour(t)=h,Month(t)=m\}|}\sum_{Hour(t)=h,Mouth(t)=m}\Delta P(t) \tag{11}$$

3.2 Historical Power-driven Rolling Ridge Regression for Day-Ahead Prediction

3.2.1 Principles of ridge regression algorithm

Ridge regression (Tikhonov regularization) addresses multicollinearity—where high feature correlation causes non-invertible data matrices—by augmenting the loss function with an L2 penalty term. This regularization enables parameter estimation when ordinary least squares fail. (Figure 2 illustrates the framework.)

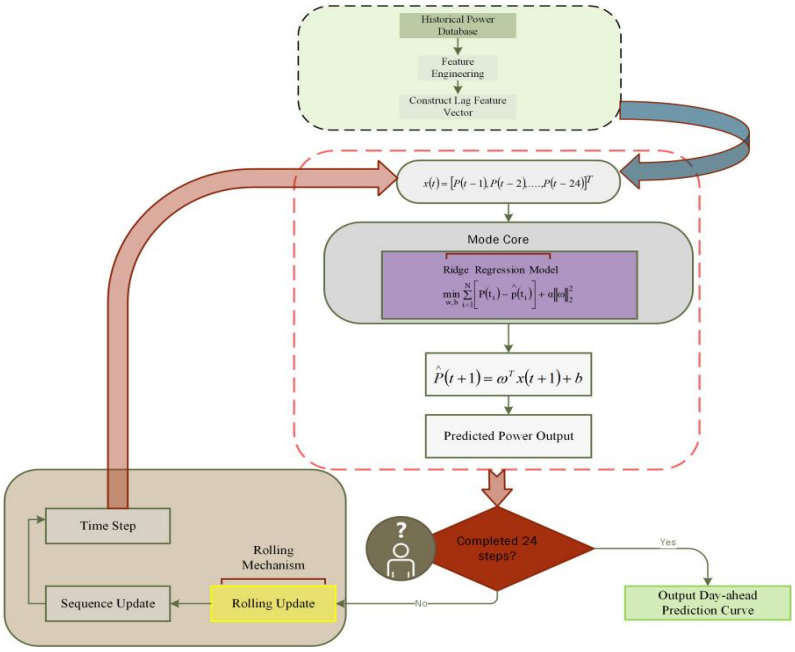

Figure 2 Schematic Diagram of the Ridge Regression Model

3.2.2 Day-ahead generation power prediction based on historical power

i) Lag feature construction. Let the actual observed power of the photovoltaic power station at time t be P(t). We use the power sequence from the past L hours as the prediction input. Construct the feature vector:

$$x(t)=[P(t-1),P(t-2),\ldots,P(t-L)]^T \tag{12}$$

where L=24 is usually taken, that is, the data from the previous 24 hours is used.

ii) The linear model based on ridge regression uses a linear regression model with L regularization, and expresses the predicted value $\hat{P}(t)$ as:

$$\hat{P}(t)=w^Tx(t)+b \tag{13}$$

where $w\in RL$ is the regression coefficient vector and b is the intercept term. The model obtains the parameters {w,b} by minimizing the following fitting loss with a regularization term:

$$min_{w,b}\sum_{i=1}^{N}\left[P(t_i)-\left(w^{\top}x(t_i)+b\right)\right]^2+\alpha//w//_2^2 \tag{14}$$

where t_i is the training sample time, and $\alpha>0$ is the regularization coefficient.

iii) Prediction and rolling window After training the parameters, perform feedback for the next 24 hours, i.e.,t=T+1,…,~T+24in sequence:

$$\hat{P}(T+1)=w^T[P(T),P(T-1),\ldots,P(T-L+1)]^T+b \tag{15}$$

then, use $\hat{P}(T+1)$as the new historical input, and repeat the process to obtain $\hat{P}(T+2)$ until $\hat{P}(T+24)$.

3.3 Scene-Adaptive Ridge Regression with Multi-Source Fusion

This model examines the meteorology-power coupling mechanism by integrating NWP and historical power data. Standardization and regularization address data heterogeneity, while irradiation-based segmented modeling enhances adaptability to sudden weather changes, overcoming single-model limitations.

3.3.1 NWP-based power generation prediction

In Mode 3, we incorporate numerical weather prediction (NWP) information based on historical power lag characteristics of the model to construct a current power generation forecast model that integrates data from multiple sources.

(1) Feature standardization and data representation in raw feature vectors

$$x(l)=[P(l-1),P(l-2),\ldots,P(l-L),N_1(l),N_2(l),\ldots,N_K(l)bigr]^T \tag{16}$$

the feature vector concatenates historical power lags (L dimensions) and NWP forecasts (K dimensions), including irradiance and meteorological variables.

Standardization is critical for this multi-source fusion: unstandardized features cause skewed weight allocation in Ridge regression due to unequal L2 penalty scaling across heterogeneous features. Z-score normalization (zero mean, unit variance) resolves this bias:

$$\bar{x}_i(t)=\frac{x_i(t)-\mu_i}{\sigma_i} \tag{17}$$

$$\mu_i=\frac{1}{N}\sum_{j=1}^{N}x_i(l_j) \tag{18}$$

$$\sigma_i=\sqrt{\frac{1}{N}\sum_{j=1}^{N}\left(x_i(l_j)-\mu_i\right)^2} \tag{19}$$

where the index i = 1, ..., K, N is the number of training samples; the standardized feature vector is denoted as $\bar{x}(t)$.μ_i is the mean of the feature value x_i on the training set,$\sigma_i$is the standard deviation of the eigenvalue x_i on the training set. This step not only improves pattern recognition speed but also avoids certain features with large dimensions causing undue bias to pattern parameters.

(2) Hyperparameter selection and cross-validation

Assume that the prediction function is linear and add L regularization to prevent overfitting. Let the pattern parameters be the weight vector w∈RL+K and the intercept b. Then, the prediction output at any time is:

$$\widehat{P}(t)=w^T\bar{x}(t)+b \tag{20}$$

Model training by minimizing the squared loss with L-regularization:

$$min_{w,b}J(w,b)=\sum_{j=1}^{N}\left[P(l_j)-\left(w^{\top}\ \bar{x}(l_j)+b\right)\right]^2+\alpha//w//_2^2 \tag{21}$$

where α > 0 is a regularization hyperparameter. To obtain the optimal weighting scheme and a model that involves fewer feature dimensions, the integrated alpha upper case I. phase can be directly compatible with regularization ,so this model is a typical quadratic convex optimization problem that can be efficiently solved using normal equations. The normal equation form is:

$$(X^TX+\alpha I)w=X^TPb=\bar{P}-w^T\bar{\bar{x}} \tag{22}$$

where $X\in RN\times(L+K)$is the feature matrix stacked with all$\bar{x}(l_j)$, and $P\in R^N$is the corresponding actual output vector, $\bar{P}$ and $\bar{x}$ are the sample mean vectors of the target and features, respectively. To avoid overfitting or underfitting, the regularization coefficient α must be optimized.

(3) Point-in-time and rolling forecasts

Hourly forecasts use the latest observed historical power and NWP forecasts to calculate $\hat{P}(t)$. once. every hour, starting at midnight on the current day. Flow must be predicted in detail on a minute-by-minute basis. This can be achieved using the following formula: At each prediction time tut, update the aging feature {P(t−1),…,P(t−L)} and call the pattern. All prediction result $\{\hat{P}(t_j)\}_{j=N+1}^{N+M}$ can be used to construct an internal power curve and compare it with actual subsequent observations.

(4) Segmented modeling approach based on weather scenarios

Although the overall model can incorporate NWP information and is helpful for smooth changes, its performance varies significantly under different weather conditions (sunny, cloudy, rainy). To further improve prediction accuracy, it is recommended to divide scenarios based on the solar radiation intensity or cloud cover forecast by NWP:

learn weather scenario: When $G_{tilt}(t)\geq\theta_{high}$ it is classified as a sunny weather model.

Partly cloudy scenario: When $\theta_{low}\leq G_{tilt}(t)<\theta_{high}$, the partly cloudy model is used.

Cloudy/rainy scenario: When $G_{tilt}(t)<\theta_{low}$,the cloudy/rainy model is adopted.

Three independent Ridge models f_{clear}、f_{cloudy}、$f_{overcast}$ are trained for the three types of samples, and during prediction, the corresponding sub-model is called after classifying the scenario based on the NWP output for the day:

$$\widehat{P}(t)=\begin{cases} f_{clear}\left(\tilde{x}(t)\right), & G_{tilt}(t)\geq\theta_{high} \\ f_{cloudy}\left(\tilde{x}(t)\right), & \theta_{low}\leq G_{tilt}(t)<\theta_{high} \\ f_{overcast}\left(\tilde{x}(t)\right), & G_{tilt}(t)<\theta_{low} \end{cases} \tag{23}$$

This segmented modeling can adopt more suitable pattern constraints for the physical and statistical characteristics of each scene, significantly improving accuracy.

3.4 A Dual-Path Spatial Downscaling Enhanced Ridge Regression Model for Photovoltaic Power Forecasting

To address NWP's kilometer-scale resolution mismatch with local microclimates, spatial downscaling via Kriging/ML generates fine-grid meteorological data, reducing prediction errors and quantifying terrain-microclimate effects for high -resolution power forecasting.

3.4.1 Downscaled NWP-based power generation prediction

In Mode 4, we compared the power prediction performance of two types of meteorological features, “original NWP” and “spatial downscaled NWP,” under the Ridge 4 framework constructed in Mode 3. The following only presents the new mathematical model expressions added in this question, without repeating the general formulas for historical lag, standardization, or evaluation indicators.

(1) NWP spatial downscaling operator Let the irradiance of the original NWP at the large-scale grid point set $\{s_j\}$be:

$$G_{tilt}(s_j,t),j=1,\ldots,J \tag{24}$$

To obtain a fine scale forecast at the precise location s_0 of the power station, this paper uses weighted spatial interpolation and a regression model:

$$\widehat{G_{tllt}^{down}}(s_0,t)=\sum_{j-1}^{J}\lambda_j G_{tilt}(s_j,t) \tag{25}$$

The weights λ_j are determined by the distance covariance model or regression coefficients, satisfying $\Sigma_j\lambda_j=1$. Similarly, other factors such as temperature and wind speed can be downscaled, denoted as $T_{air}^{down}(t),W_s^{down}(t)$ The downscaling error is ε(t). We have:

$$G_{tilt}^{down}(s_0,t)=G_{inlt}(s_0,t)+\varepsilon(t) \tag{26}$$

(2) Feature vector expansion Based on the historical lag vector p(t), the original NWP features are:

$$n^{orig}(t)=|G_{tilt}(t),T_{air}(t),W_s(t)|^T \tag{27}$$

where $n^{orig}(t)$ is the weather forecast for the original NWP.

After downscaling, the characteristics are as follows:：

$$n^{down}(t)=\left[G_{tilt}^{down}(t),T_{air}^{down}(t),W_s^{down}(t)\right]^T \tag{28}$$

where $n^{down}(t)$ is the NWP weather forecast after downscaling.

The two inputs are concatenated to obtain the complete feature vector:

$$x^{orig}(t)=\begin{bmatrix}p(t)\\ n^{orig}(t)\end{bmatrix} \tag{29}$$

where $x^{orig}(t)$ is the original complete feature vector.

$$x^{down}(t)=\begin{bmatrix}p(t)\\ n^{down}(t)\end{bmatrix} \tag{30}$$

where $x^{down}(t)$ is the complete eigenvector after downscaling.

(3) Ridge four regression prediction model

Train a linear regression with regularization for each of the two sets of features:

$$\widehat{P^{(k)}}(l)=w^{(k)T}\tilde{x}^{(k)}(l)+b^{(k)},k\in\{orig,down\} \tag{31}$$

where $\bar{x}^{(k)}$ is the normalized feature vector, and the parameters {w(k),b(k)} are obtained by minimizing the regularized squared error:

$$min_{w,b}\sum_{j=1}^{N}\left[P(t_j)-\left(w^T\bar{x}(t_j)+b\right)\right]^2+\alpha\|\omega\|_2^2 \tag{32}$$

(4) Define the downscaling improvement quantity as:

$$\Delta MAE=MAE^{(down)}-MAE^{(orig)} \tag{33}$$

$$\Delta R^2=R^{2(down)}-R^{2(orig)} \tag{34}$$

if $\Delta MAE<0$ and $\Delta R^2>0$， it indicates that downscaling effectively improves accuracy; Otherwise, there is no gain, or it causes damage.

4 PHOTOVOLTAIC POWER PREDICTION MODEL SOLUTION AND ANALYSIS

The data in this article comes from www.selectdataset.com.

4.1 Results and analysis corresponding to Spatiotemporal Performance Diagnostic Model for PV Plants

In this section, we quantify the seasonal and cyclical intraday generation power characteristics through monthly, intraday, and two-dimensional matrices to provide a theoretical basis for subsequent power prediction revisions and system performance optimization.

4.1.1 Heat map of intraday and monthly average deviation of cleaned data

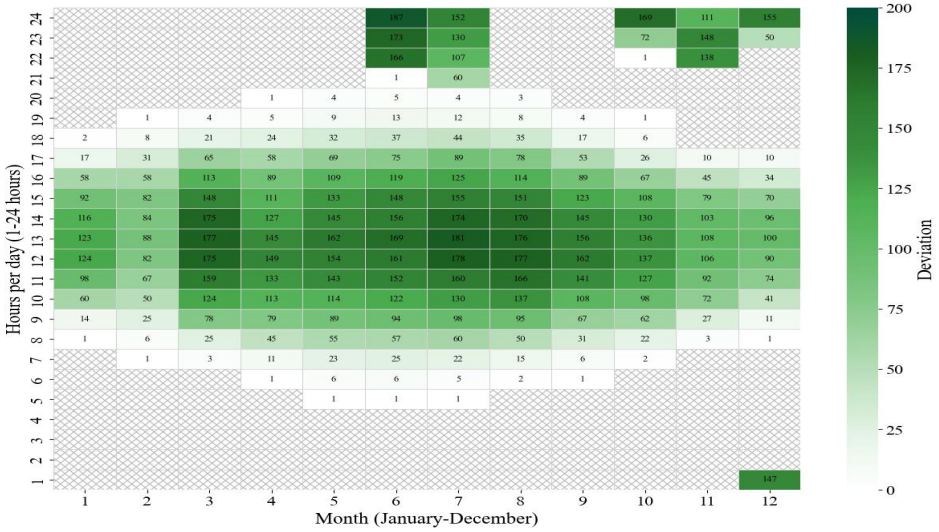

Figure 3 Heat Map of Average Deviation of Cleaned Data

The Figure 3 show deviations peak during midday/summer due to high irradiation and temperature, with minimal morning/dusk/winter fluctuations, revealing month-dependent efficiency loss patterns.

4.1.2 Analysis of model results

Table 1 Key Indicator Analysis Table for Model One

Serial number	Indicator	Numerical value
1	MAE	87.845167
2	RMSE	112.459885
3	Pearson correlation coefficient	0.951533

Table 1 shows good but imperfect alignment between actual and predicted power， systematically quantifies PV plant deviations from theoretical irradiation models, revealing spatiotemporal patterns and meteorological constraints. These unexplained errors necessitate historical power-based day-ahead prediction models to capture dynamic features for enhanced accuracy.

4.2 Corresponding results and analysis of Spatiotemporal Performance Diagnostic Model for PV Plants

In this section, the Ridge model is utilized to perform rolling forecasts by training the past 24 hours' eigenvalues, which are used to validate the accuracy of the historical power-based PV power prediction model.

4.2.1 Comparison chart of forecast time series in the past few days

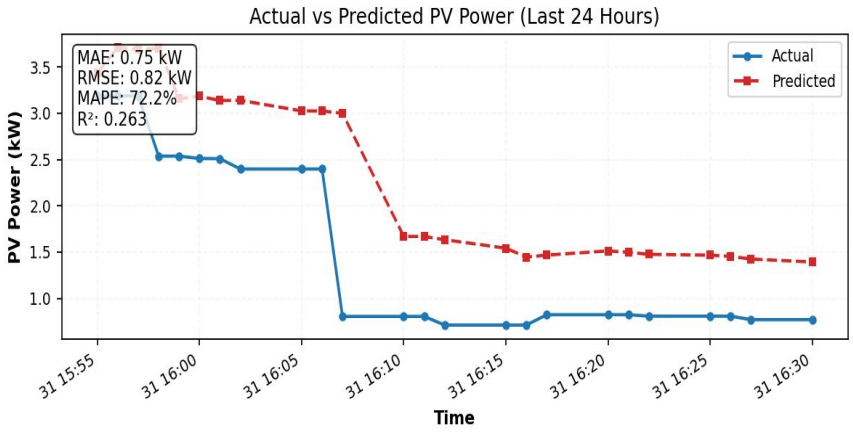

Figure 4 Comparison Chart of Predicted Values and Actual Values over the Past 24 Hours

Figure 4 demonstrates the timing of the Ridge model's 24-hour prediction results based on historical power compared to actual power. The overall trend of the prediction curves matches, but there is a significant lag during the sudden weather change hours, indicating that the pure historical power model is difficult to capture the meteorologically driven transient fluctuations and needs to be supplemented with external information.

4.2.2 Analysis of model results

Table 2 Key Indicator Analysis Table for Mode 2

Serial number	Indicator	Numerical value
1	MAE	0.750148
2	RMSE	0.824839
3	MAPE	72.193061
4	R^2	0.2633358

Table 2 Key Indicator Analysis Table for Mode 2shows that there is a weak correlation between historical power models and weather-induced peak forecast lags, which requires integration with numerical weather prediction (NWP) to improve adaptability to sudden weather events. This prompted us to construct a hybrid 'historical' model to quantify the value of meteorological information in forecasting.

4.3 Results and Analysis of Scene-Adaptive Ridge Regression with Multi-Source Fusion

In this section, a prediction model for day-ahead power generation of PV plants incorporating NWP information is developed to compare with the previous prediction based on historical power and to test whether the incorporation of NWP is conducive to the improvement of prediction accuracy.

4.3.1 Timing comparison chart for fusion NWP

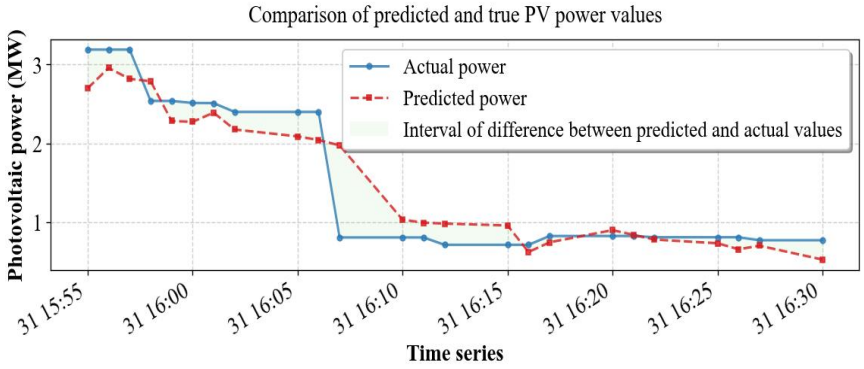

Figure 5 Comparison Analysis Chart between NWP-based Forecasts and Actual Time Series

The time series diagram after introducing NWP is shown in Figure 5 Comparison analysis chart between NWP-based forecasts and actual time series. Compared with the previous experiment, the conclusion that the lag phenomenon is alleviated after introducing numerical weather prediction (NWP) is relatively intuitive. However, the coefficient of determination R^2 value is between 0.5 and 0.8, indicating a moderate level of correlation. Therefore, based on this result, there is still room for improvement in prediction accuracy.

4.3.2 Analysis of model results

Table 3 Key Indicator Analysis Table for Model 3

Serial number	Indicator	Numerical value
1	MAE	0.462041
2	RMSE	0.566169
3	R^2	0.652935
4	MAPE	49.178673

The results are shown in Table 3. Key Indicator Analysis Table for Model 3. Although numerical weather prediction (NWP) can improve forecast accuracy under stable weather conditions, its low spatial resolution limits its ability to forecast cloudy/rainy scenarios. Therefore, spatial downscaling techniques are needed to refine local weather forecasts and overcome the current limitations of NWP accuracy.

4.4 Results and Analysis of a Dual-Path Spatial Downscaling Enhanced Ridge Regression Model for Photovoltaic Power Forecasting

This study addresses NWP's kilometer-scale resolution limitations for PV plants by developing a downscaling algorithm to generate localized forecasts. Error comparisons (peak deviation/distribution) validate enhanced accuracy of downscaled predictions.

4.4.1 Comparison of time series before and after downscaling

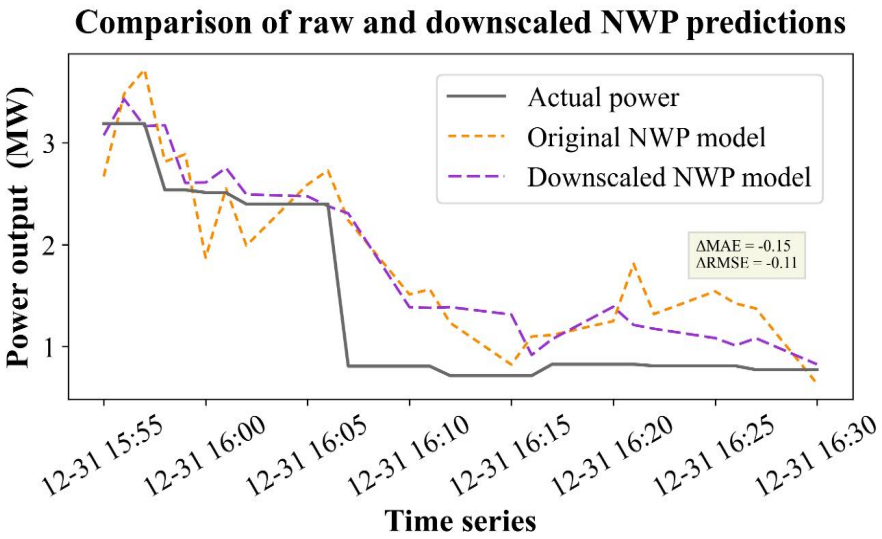

Figure 6 Comparison Analysis Chart of Time Series Data from the Original and Downscaled NWP Models

The time series diagrams before and after downscaling are shown in Figure 6. By comparing the time series before and after downscaling, it can be seen that the numerical weather prediction (NWP) results after downscaling are closer to the actual power curve, especially during periods of rapid changes in irradiance intensity.

4.4.2 Distribution of point clouds before and after downscaling

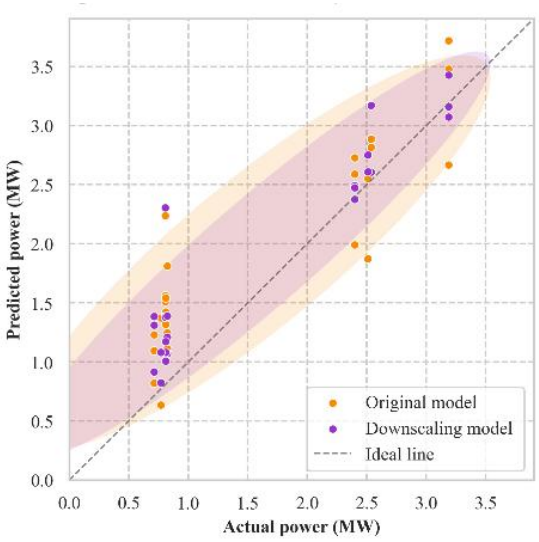

(a) Scattered Comparison of Prediction Accuracy Based on Downscaled NWP Models

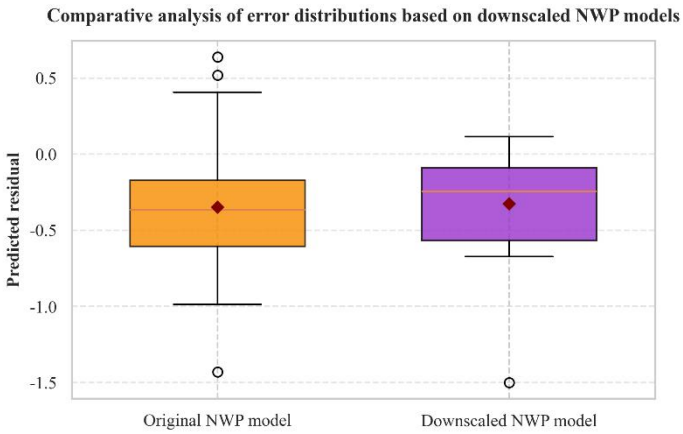

(b) Comparative analysis of error distributions based on downscaled NwP models

Figure 7 Point Cloud Distribution and Residual Distribution Feature Maps of Original and Scaled NWP Models

The fitting results before and after downscaling, as well as the residual distribution, are shown in Figure 7. The downscaled version not only reduced the error but also lowered the mean absolute error (MAE) to 0.34, the root mean square error (RMSE) to 0.46, and improved the correlation coefficient (R) to 0.76. This indicates that downscaling simulations using simple random perturbations filtered out some additional noise, improving the model's predictive capability and yielding point cloud distribution feature maps.

4.4.3 Analysis of model results

Table 4 Comparison table of Indicators for Original NWP and Downscaled NWP Models

Indicator value	MAE	RMSE	R^2
Downscaling NWP	0.339345	0.465706	0.765175
Original NWP	0.490388	0.573204	0.644256

The final results are shown Table 4 Comparison table of indicators for original NWP and downscaled NWP models. From a quantitative perspective, the Ridge regression model performed excellently under the original numerical weather prediction (NWP) characteristics: the mean absolute error (MAE) was approximately 0.34, the root mean square error (RMSE) was approximately 0.47, and the correlation coefficient (R) was approximately 0.77. This indicates that large-scale weather forecasts can accurately describe the overall trend and daily changes in electricity demand.

5 CONCLUSION AND OUTLOOKS

The final results are shown in Table 4. From a quantitative perspective, the Ridge regression model performed excellently under the original numerical weather prediction (NWP) characteristics: the mean absolute error (MAE) was approximately 0.34, the root mean square error (RMSE) was approximately 0.47, and the correlation coefficient (R) was approximately 0.77. This indicates that large-scale weather forecasts can accurately describe the overall trend and daily changes in electricity demand.

Future research will focus on: i) Integrating higher-resolution satellite cloud imagery with ground-based sky imaging data to enhance the ability to capture cloud dynamics; ii) Exploring the deep integration of deep learning with physical mechanism models to enhance the robustness of extreme weather forecasting; iii) Evaluating the framework's generalisation performance across diverse climate regions and large-scale power plant clusters; iv) Deepening the application value of prediction results in power market transactions, energy storage optimisation scheduling, and virtual power plant operations, providing stronger decision-making support for the safe, economical, and low-carbon operation of grids with high proportions of renewable energy.

COMPETING INTERESTS

The authors have no relevant financial or non-financial interests to disclose.

REFERENCES

[1] Sharadga H, Hajimirza S, Balog R S. Time series forecasting of solar power generation for large-scale photovoltaic plants. Renewable Energy, 2020, 150: 797-807.

[2] Luo X, Zhang D, Zhu X. Deep learning-based forecasting of photovoltaic power generation by incorporating domain knowledge. Energy, 2021, 225: 120240.
[3] Wang J, Zhou Y, Li Z. Hour-ahead photovoltaic generation forecasting method based on machine learning and multi objective optimization algorithm. Applied Energy, 2022, 312: 118725.
[4] Radhi S M, Al-Majidi S D, Abbod M F, et al. Machine Learning Approaches for Short-Term Photovoltaic Power Forecasting. Energies, 2024, 17(17): 4301.
[5] Guo X, Mo Y, Yan K. Short-term photovoltaic power forecasting based on historical information and deep learning methods. Sensors, 2022, 22(24): 9630.
[6] Zhang R, Wu Y, Zhang L, et al. A multiscale network with mixed features and extended regional weather forecasts for predicting short-term photovoltaic power. Energy, 2025: 134792.
[7] Seshadri P, TS B P, S S. Time Series-Based Photovoltaic Power Forecasting to Optimize Grid Stability. Electric Power Components and Systems, 2021, 49(16-17): 1379-1388.
[8] Ding S, Li R, Tao Z. A novel adaptive discrete grey model with time-varying parameters for long-term photovoltaic power generation forecasting. Energy Conversion and Management, 2021, 227: 113644.
[9] Ilias L, Sarmas E, Marinakis V, et al. Unsupervised domain adaptation methods for photovoltaic power forecasting. Applied Soft Computing, 2023, 149: 110979.
[10] Zhang X, Yu T, Yang B, et al. A random forest-assisted fast distributed auction-based algorithm for hierarchical coordinated power control in a large-scale PV power plant. IEEE Transactions on Sustainable Energy, 2021, 12(4): 2471-2481.